Supporting information

Edge-rich and Dopant-free Graphene as Highly Efficient Metal-free Electrocatalyst for Oxygen Reduction Reaction

Li Tao, Qiang Wang, Shuo Dou, Zhaoling Ma, Jia Huo, Shuangyin Wang* and Liming Dai*

Email: shuangyinwang@hnu.edu.cn (S. Wang)
liming.dai@case.edu (L. Dai)

Experimental Section

Material preparation

Graphene oxide (GO) was synthesized from flaky graphite powder by a modified Hummers method. In brief, 5 g of crystalline flake graphite and 150 ml of concentrated sulfuric acid were put into a round-bottom flask and stirred for 1 h at 0 ℃. Then, 25 g of potassium permanganate was gradually added to obtain a black-green solution which was continuously stirred for 45 min. The product was then further treated by adding of 150 ml of ultrapure water for 0.5 h stirring at 38 ℃, followed by the addition of 38 ml 30 % hydrogen peroxide. The mixture slurry was then washed with diluted hydrochloric acid and ultrapure water until the supernatant solution obtained the pH of 7. After freeze-drying, the graphene was annealed in 800℃ to remove the surface oxygenic functional groups. Then 40 mg graphene was put in a quartz boat. Ar plasma (commercial 13.56 MHz RF source) with power of 300 W and pressure of 40 Pa is used to treat the graphene with different irradiation time and temperature.

Characterazition

X-ray powder diffraction (XRD) was carried out on a Siemens D500 diffractometer with a Cu Kα source (1.54056Å). Diffraction data were collected for 2θ angles from 10° to 90° at a scan rate of 5 °/ min. The morphology and microstructure of the graphene were investigated by scanning electron microscope (SEM, Hitachi, S-4800) and transmission electron microscopy (TEM, JEM-2100F). The Raman spectra were recorded at room temperature on a Horiba HR 800 with an argon ion laser operating at 632 nm. X-ray photoelectron spectroscopy (XPS) measurements and analysis were recorded on a Thermo Fisher-VG Scientific (ESCALAB 250Xi) photoelectron spectrometer.

Electrochemical measurement

Electrochemical measurements of graphene for ORR were conducted at room temperature in a standard three-electrode cell on a CHI760E (CH Instrument, USA) electrochemical workstation and d a rotating ring disk electrode apparatus (RRDE-3A, ALS, Japan) , with a 0.1 M KOH solution was used as the electrolyte, A glassy carbon electrode (4 mm in diameter) was used as the working electrode; a large surface area Platinum mesh (1 cm×1 cm) and saturated calomel electrode (SCE) were used as the counter and reference electrode, respectively. 4 mg of catalyst was dispersed in 2 ml ethanol and ultrasonicated for 1 h, then, 100 µl of 5 wt% Nafion solution (5 wt%, Sigma Aldrich, USA) was added into the slurry followed by ultrasonication for anther 1h. After that, the working electrode was coated with 10 µL of the above catalyst ink, and dried naturally. All potentials were converted to the reversible hydrogen electrode (RHE) to unequivocally compensate for the pH changes.

Koutecky-Levich equation:

$$\frac{1}{j} = \frac{1}{j_k} + \frac{1}{B\omega^{0.5}}$$

Where j_k is the kinetic current and ω is the electrode rotating rate. B was calculated based on the Levich equation from the slope of the *K–L* plots (Figure. 3d) as follows:

$$B = 0.2nF\,(D_{O_2})^{\frac{2}{3}}\,v^{-1/6}C_{O_2}$$

Where n is the electrons transfer number per oxygen molecule, F is the Faraday constant (F=96485 C mol^{-1}), D_{O_2} is the diffusion coefficient of O_2 in 0.1 M KOH (1.9×10^{-5} cm^2 s^{-1}) and v and C_{O_2} are the kinetic viscosity (0.01 cm^2 s^{-1}) and bulk concentration of O_2 (1.2×10^{-6} mol cm^{-3}), respecitvely. The constant 0.2 is adopted when the rotation speed is expressed in *rpm*.

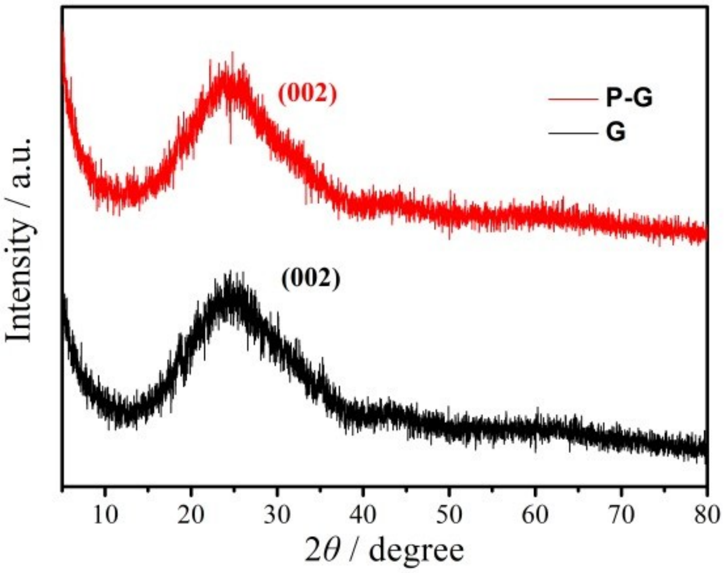

Figure S1. XRD patterns of pristine graphene and Plasma treated graphene.

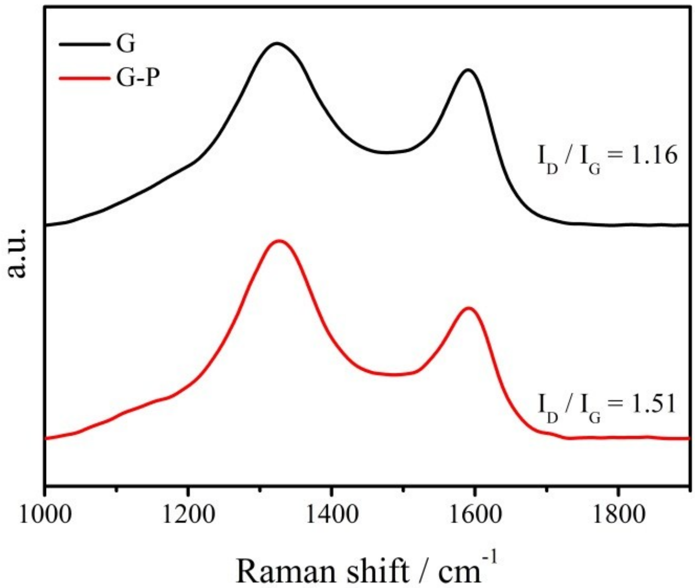

Figure S2.Raman characterizations of G and G-P.

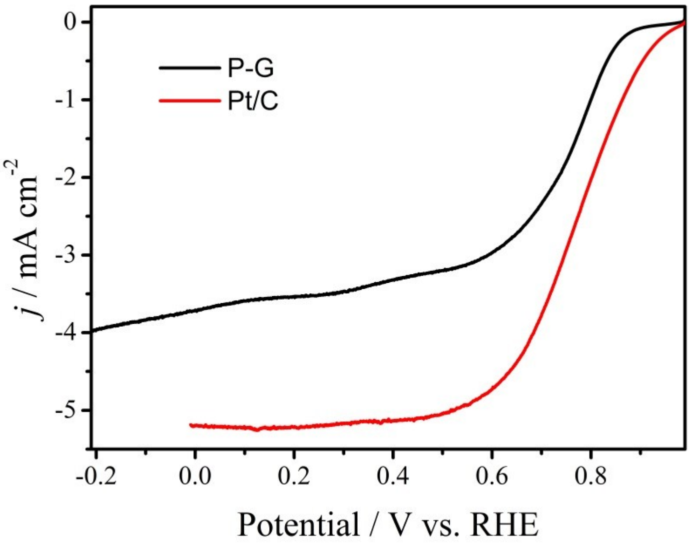

Figure S3. Rotating disk electrode (RDE) voltammograms of P-G and Pt/C in an O_2-saturated 0.1 M KOH solution with a scan rate of 10 mV s^{-1}.

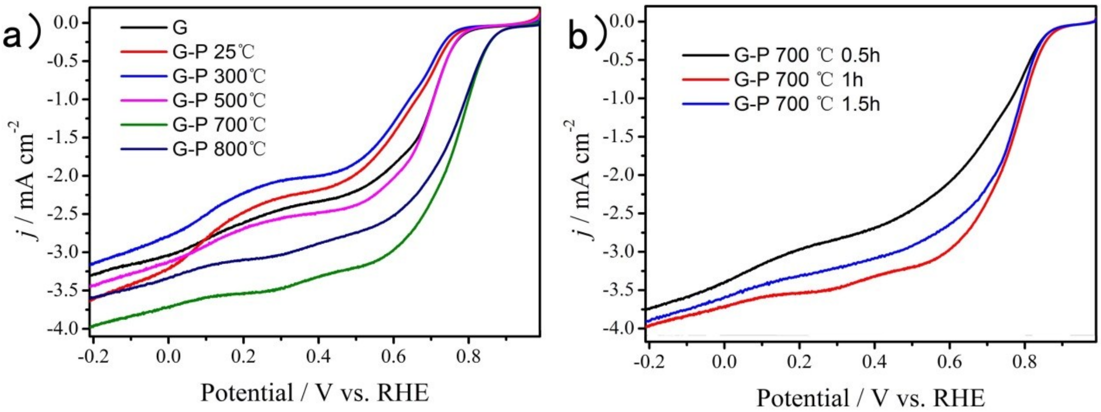

Figure S4. RDE voltammograms of plasma treated graphene with different temperature (a) and at 700 ℃ with different time in an O_2-saturated 0.1 M aqueous KOH solution with a scan rate of 10 mV s^{-1} at a constant rotation rate of 1600 rpm.

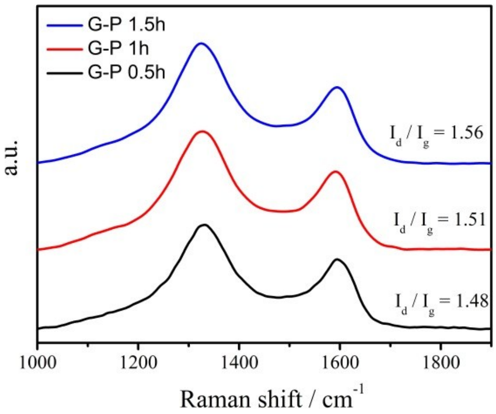

Figure S5. Raman characterizations of plasma treated graphene at 700 ^{o}C with different time.

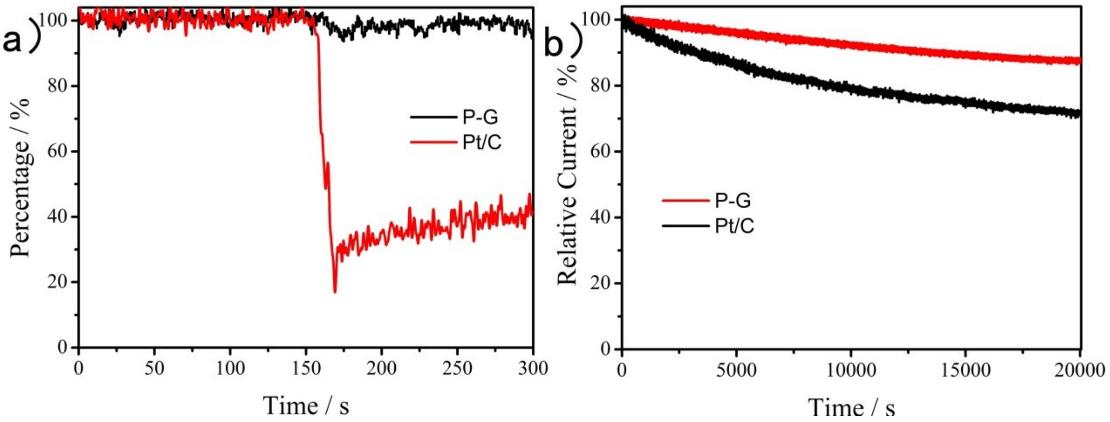

Figure S6. The current-time (i-t) chronoamperometric responses for ORR at the P-G and Pt/C electrodes in an O_2-saturated 0.1 M KOH solution at 0.74 V versus RHE 3.0 M, methanol was added at around 150 s. Durability evaluation of P-G and Pt/C electrodes for 20 000 s at 0.74 V versus RHE.

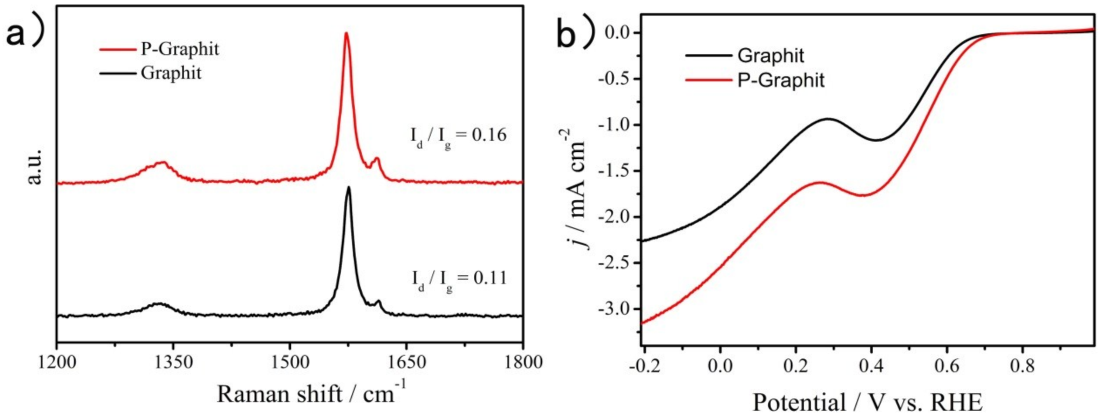

Figure S7.Raman characterizations of CNT and P-CNT (a); RDE voltammograms of pristine and plasma treated edge-rich carbon nanotubes in an O_2-saturated 0.1 M aqueous KOH solution with a scan rate of 10 mV s^{-1}(b);

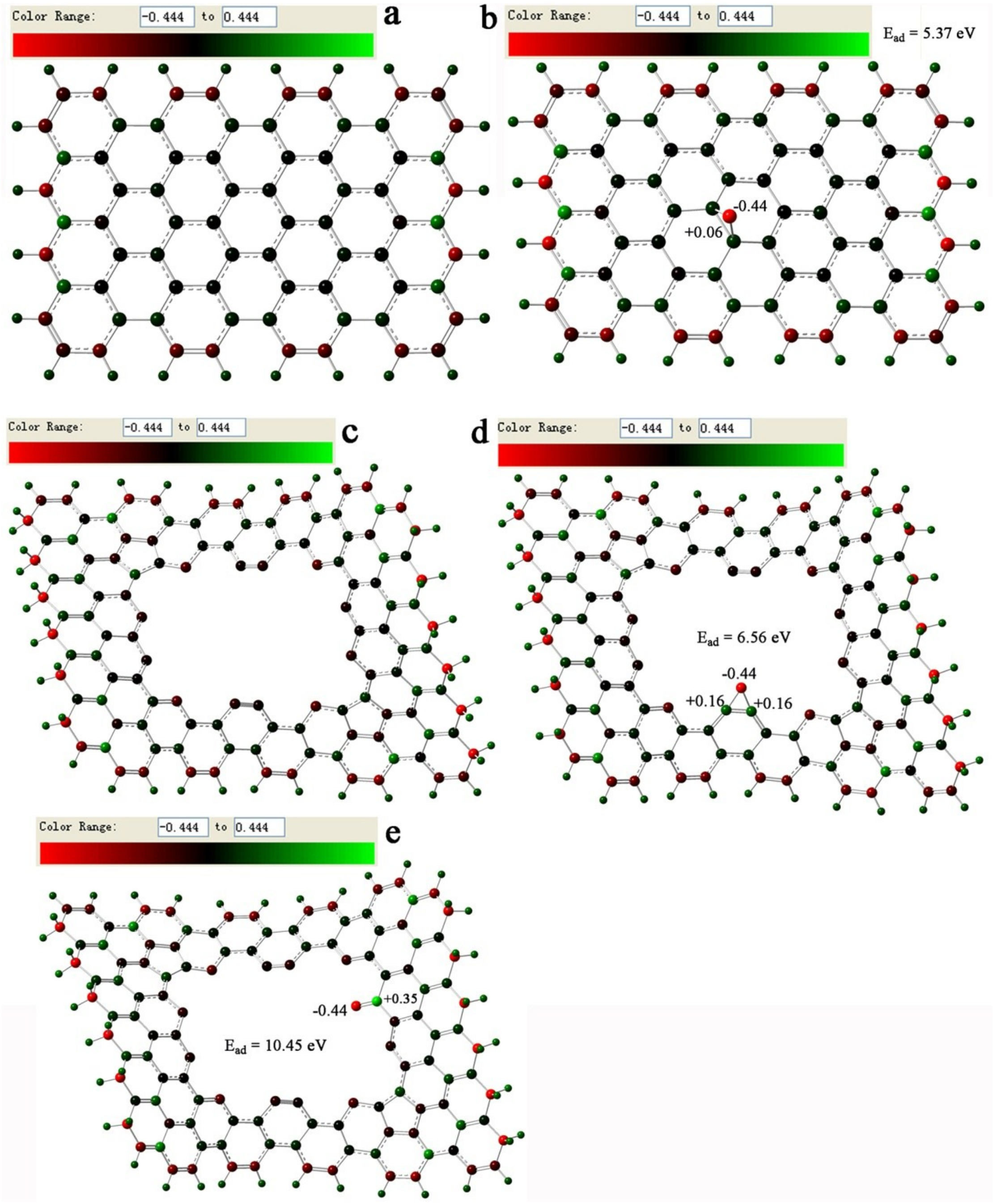

Figure S8. Charge distribution on the (a) perfect graphene sheet of $C_{72}H_{24}$, (b) O-adsorbed $C_{72}H_{24}$-O system, (c) defective graphene sheet of $C_{122}H_{46}$, (d) and (e) O-adsorbed $C_{122}H_{46}$-O systems with different defect adsorbed site.

The perfect and defective graphene sheets and their O-adsorbed graphene-O systems were built, respectively, as shown in Figure S6. Carbon atoms on the edge of the graphene sheets are terminated by hydrogen atoms. The calculations were carried out using Gaussian09 program package (revision B.01; Gaussian, Inc., Wallingford CT, 2010.).[11] The geometries of two graphene sheets were fully optimized at B3LYP/6-31G (d,p)[12-16] level. The adsorption energy of O atom on graphene surface or the edge of graphene defect is calculated using $\Delta E_{ad} = E_{g\text{-}O} - (E_{sp/g}+E_{sp/O})$, where ΔE_{ad} and $E_{g\text{-}O}$ are the adsorption energy and total energy of the graphene-O system, $E_{sp/g}$ and $E_{sp/O}$ are the single point energies of the separated O atom and graphene sheet. The geometric structures of the separated O atom and graphene sheet were kept the same as those in the graphene-O system, respectively.

Table S1. Distribution of C species obtained from the de-convolution of the C1s peaks by XPS.

	sp^2	*sp*^{3}	C-O	C=O	π-π*
G	71.80%	11.65%	3.09%	5.49%	7.95%
P-G	72.04%	14.11%	2.42%	2.92%	8.49%

Table S2. Comparison of oxygen reduction reaction on P-G and other metal-free carbon materials in literatures with the similar testing conditions.

Materials	mass loading μg cm^{-2}	electrolyte	Reference electrode	on-set potential	n[a]	Ref
G-P	160	0.1 M KOH	RHE	0.912 V	3.85	--
Nitrogen-doped graphene	141	0.1 M KOH	Ag/AgCl	-0.18 V	3.5-4.0	1
Doped graphene quantum dots	283	0.1 M KOH	Ag/AgCl	-0.16 V	3.6-4.4	2
Edge-selectively sulfurized graphene nanoplatelets	76	0.1 M KOH	Ag/AgCl	-0.22 V	3.3	3
N and O doped mesoporous carbons	100	0.1 M KOH	RHE	0.94 V	3.78	4
Nitrogen-doped carbon nanotubes	28	0.1 M KOH	Hg/HgO	-0.15 V	~3.0	5
Nanoporous graphitic-C_3N_4@carbon	283	0.1 M KOH	Ag/AgCl	-0.10 V	4.0	6
Polyelectrolyte-functionalized graphene	--	0.1 M KOH	SCE	-0.12 V	3.5-4.0	7
Molecular doping of graphene	160	0.1 M KOH	SCE	-0.204 V	3.1	8
Phosphorus-Doped Graphene	51	0.1 M KOH	RHE	0.92 V	3.0-3.8	9
N,S,O-doped ordered mesoporous carbons	159	0.1 M KOH	RHE	0.85 V	3.5	10

[a] Electron transferred number for ORR.

Reference:

1. Z. Lin, G. Waller, Y. Liu, M. Liu and C.-P. Wong, Advanced Energy Materials, 2012, 2, 884-888.
2. Y. Li, Y. Zhao, H. Cheng, Y. Hu, G. Shi, L. Dai and L. Qu, J. Am. Chem. Soc., 2012, 134, 15-18.
3. J. In-Yup, Z. Sheng, Z. Lipeng, C. Hyun-Jung, S. Jeong-Min, X. Zhenhai, D. Liming and B. Jong-Beom, Adv. Mater., 2013, 25, 6138-6145.
4. S. Rafael, V. Damien, C. Manish and A. Tewodros, J.am.chem.soc, 2013, 135, 7823-7826.
5. T. Sharifi, G. Hu, X. Jia and T. Wågberg, Acs Nano, 2012, 6, 8904-8912.
6. Z. Yao, J. Yan, C. Jun, L. Jian, L. Ji, D. Aijun, Z. Weimin, Z. Zhonghua, S. C. Smith and J. Mietek, J. Am. Chem. Soc., 2011, 133, 20116-20119.
7. S. Wang, D. Yu, L. Dai, W. C. Dong and J. B. Baek, Acs Nano, 2011, 5, 6202-6209.
8. D. Shuo, S. Anli, T. Li and W. Shuangyin, Chem. Commun., 2014, 50, 10672-10675.
9. C. Zhang, N. Mahmood, H. Yin, F. Liu and Y. Hou, Adv. Mater., 2013, 25, 4932-4937.
10. J. Y. Cheon, J. H. Kim, J. H. Kim, K. C. Goddeti, J. Y. Park and S. H. Joo, J. Am. Chem. Soc., 2014, 136, 8875−8878.
11. M. J. Frisch, G. W. Trucks, H. B. Schlegel, G. E. Scuseria, M. A. Robb, J. R. Cheeseman, G. Scalmani, V. Barone, B. Mennucci, G. A. Petersson, H. Nakatsuji, M. Caricato, X. Li, H. P. Hratchian,
12. A. F. Izmaylov, J. Bloino, G. Zheng, J. L. Sonnenberg, M. Hada, M. Ehara, K. Toyota, R. Fukuda, J. Hasegawa, M. Ishida, T. Nakajima, Y. Honda, O. Kitao, H. Nakai, T. Vreven, J. A. Montgomery, Jr., J. E. Peralta, F. Ogliaro, M. Bearpark, J. J. Heyd, E. Brothers, K. N. Kudin, V. N. Staroverov, T. Keith, R. Kobayashi, J. Normand, K. Raghavachari, A. Rendell, J. C. Burant, S. S. Iyengar, J. Tomasi, M. Cossi, N. Rega, J. M. Millam, M. Klene, J. E. Knox, J. B. Cross, V. Bakken, C. Adamo, J. Jaramillo, R. Gomperts, R. E. Stratmann, O. Yazyev, A. J. Austin, R. Cammi, C. Pomelli, J. W. Ochterski, R. L. Martin, K. Morokuma, V. G. Zakrzewski, G. A. Voth, P. Salvador, J. J. Dannenberg, S. Dapprich, A. D. Daniels, O. Farkas, J. B. Foresman, J. V. Ortiz, J. Cioslowski, and D. J. Fox, Gaussian, Inc., Wallingford CT, 2010.
13. Ditchfield, R.; Hehre, W. J.; Pople, J. A. J. Chem. Phys. 1971, 54, 724–728.
14. Hehre, W. J.; Ditchfield, R.; Pople, J. A. J. Chem. Phys. 1972, 56, 2257–2261.
15. Hariharan, P. C.; Pople, J. A. Theor. Chem. Acc. 1973, 28, 213–222.
16. Francl, M. M.; Pietro, W. J.; Hehre, W. J.; Binkley, J. S.; DeFrees, D. J.; Pople, J. A.; Gordon, M. S. J. Chem. Phys. 1982, 77, 3654–3665.